Calculation of flow-induced residual stresses in injection molded products

Applied Scientific Research **48**: 141–157, 1991.

Calculation of flow-induced residual stresses in injection moulded products

FRANK P.T. BAAIJENS & LUCIEN F.A. DOUVEN*

*Philips Research Laboratories, P.O. Box 80000, 5600 JA Eindhoven, The Netherlands; *Eindhoven University of Technology, Faculty of Mechanical Engineering, Section of Engineering Fundamentals, P.O. Box 513, 5600 MB Eindhoven, The Netherlands*

Received 4 July 1990; accepted in revised form 3 November 1990

Abstract. Flow-induced residual stresses that arise during the injection moulding of amorphous thermoplastic polymers are calculated in both the filling and post-filling stage. To achieve this a compressible version of the Leonov model is employed. Two techniques are investigated. First a direct approach is used where the pressure problem is formulated using the viscoelastic material model. Secondly, generalized Newtonian material behaviour is assumed, and the resulting flow kinematics is used to calculate normal stresses employing the compressible Leonov model. The latter technique gives comparable results, while reducing the computational cost significantly.

Nomenclature

a = scalar
$\mathbf{a}$ = vector
$\mathbf{A}$ = tensor
$\mathbf{A}^c$ = conjugate of $\mathbf{A}$
$\mathbf{A}^d$ = deviatoric part of $\mathbf{A}$
$\mathbf{a}.\mathbf{a}$ = dot product of two vectors
$\mathbf{a}.\mathbf{A}$ = dot product of vector with second order tensor
$\mathbf{ab}$ = dyadic product
$\mathbf{A}.\mathbf{B}$ = dot product of two second order tensors
$\mathrm{tr}(\mathbf{A})$ = trace of $\mathbf{A}$
$\mathbf{A}:\mathbf{B}$ = trace of $\mathbf{A}.\mathbf{B}$
$\det(\mathbf{A})$ = determinant of $\mathbf{A}$
$(\underline{\ })$ = column
$(\underline{\ })^T$ = transpose of a column
$(\underline{\underline{\ }})$ = matrix
$(\dot{})$ = material time derivative
$(\dot{})_e$ = elastic part of $(\dot{})$
$(\dot{})_p$ = plastic part of $(\dot{})$

$\dot{\gamma}$ = shear rate
ε = specific internal energy
λ = heat conduction coefficient
θ = relaxation time
η = viscosity
ρ = density
v = specific volume
a_T = time-demperature shift factor
c_p = specific heat at constant pressure
J = volume change factor
N_1 = first normal stress difference
p = pressure
r = internal heat source
∇ = gradient operator with respect to current configuration
∇_0 = gradient operator with respect to reference configuration
$\mathbf{h}$ = heat flux
$\mathbf{v}$ = velocity
$\mathbf{x}$ = position vector
$\boldsymbol{\sigma}$ = Cauchy stress tensor
$\boldsymbol{\tau}$ = extra stress tensor
$\mathbf{D}$ = rate of strain tensor
$\mathbf{F}$ = deformation tensor
$\mathbf{B}$ = left Cauchy–Green tensor
$\mathbf{L}$ = velocity gradient tensor

1. Introduction

Injection moulding is a commonly applied processing technology for plastics. In the past decade, attention in numerical simulations of the injection moulding process has been focused on the filling stage. The key items in these calculations are the prediction of pressure and temperature distributions and the progression of the flow front in complex-shaped, thin-walled geometries. Numerous commercial codes are available nowadays, e.g. Boshouwers and v.d. Werf [1], Sitters [2] and Manzione [3].

More recently, the prediction of residual stresses (and molecular orientation) in injection moulded products has attracted attention. Knowledge of residual stresses is essential to predict dimensional and shape inaccuracies of a product. Roughly, there are two sources of residual stresses. First, due to the viscoelastic nature of the polymeric melt, normal stresses develop during the filling, packing and holding stage. Usually, these so-called flow-induced stresses are relatively small. However they give rise to large molecular orientations which affect the mechanical and optical (birefringence) behaviour of a product. They also give rise to differences in (post-) shrinkage behaviour in directions perpendicular and parallel to the flow direction. The second cause of residual stresses is the rapid increase in rigidity of the material as it passes through the glass transition point (or region). Across the product wall a highly non-uniform temperature distribution exists. Therefore each material point solidifies at a different time, leading to differential shrinkage causing thermally induced stresses.

Initial investigations by Isayev and Hieber [4] show the potential capabilities of the so-called Leonov model, first published by Leonov [5], to predict flow-induced residual stresses during the filling-stage. Birefringence measurements of Wimberger-Friedl and Janeschitz-Kriegl [13] in Compact Discs and Isayev and Hariharan [15] indicate that molecular orientation is not only introduced during the filling but also during the post-filling (packing and holding) stage of the injection moulding process. The traditional incompressible version of the model as applied by Isayev and Hieber [4] is slightly modified to include compressibility effects; an essential feature in the packing stage. By following Stickforth [6] and Simo [7], a kinematic split of the elastic deformation tensor into a volumetric and a deviatoric part is defined and a compressible version of the Leonov model is derived. As the model reduces to that of a linear viscoelastic medium for small deformations, only linear viscoelastic measurements are required to determine the material properties.

Two approaches are investigated to calculate flow induced residual stresses by means of the compressible Leonov model. Firstly, the viscoelastic material behaviour is taken into account to derive the so-called pressure problem (Sitters [2]). This is called the *direct* approach. Secondly an *indirect* method is developed, where the pressure problem is derived employing a generalized Newtonian model, while the resulting flow kinematics is used as input for the viscoelastic constitutive equation to calculate flow induced residual stresses. The latter approach reduces computational time considerably.

2. Governing equations

The three dimensional governing equations are:

1. Continuity equation, representing the conservation of mass

$$\frac{\dot{\rho}}{\rho} + \mathbf{V}.\mathbf{v} = 0 \tag{2.1}$$

where ρ represents the density (the inverse of the specific volume v), $\mathbf{V}$ the gradient operator, and $\mathbf{v}$ the velocity field.

2. The momentum equation

$$\mathbf{V}.\boldsymbol{\sigma} + \rho\mathbf{f} = \rho\mathbf{v} \tag{2.2}$$

where $\boldsymbol{\sigma}$ is the Cauchy stress tensor and $\mathbf{f}$ the body force per unit mass.

3. The energy equation

$$\rho\dot{\varepsilon} = \boldsymbol{\sigma}:\mathbf{D} - \mathbf{V}.\mathbf{h} + \rho r \tag{2.3}$$

where ε is the specific internal energy, $\mathbf{D}$ the rate of deformation tensor, $\mathbf{h}$ the heat flux and r an internal heat source.

This set of equations can not be solved as such, constitutive equations for the density, the Cauchy stress tensor, the specific internal energy, the heat flux and the internal heat source must be given, accompanied by appropriate initial and boundary conditions. This is the object of the next section.

However, some remarks can be made here. First, due to the extremely high viscosity of the material compared to the velocities, inertia effects are neglected in the momentum equation. Body forces can be neglected and no internal heat source is assumed to be present. Further, solving the full three dimensional theory would be highly uneconomical, and would bypass the typical geometrical properties of the product, such as narrowness and weakly curvedness. With a few suitably chosen kinematical assumptions a much more workable theory is derived.

3. Constitutive models

3.1. The compressible Leonov model

Constitutive models are given to describe the thermodynamic behaviour of isotropic amorphous polymers. First a model is presented to characterise the thermo-mechanical behaviour. Thereafter, thermal properties are briefly discussed.

The mechanical behaviour in shear dominated flows (as in injection moulding) can be described reasonably well with the so-called Leonov model, as shown by for example, Upadyay et al. [8]. During the filling stage, compressibility effects may be neglected, as opposed to the post-filling stage where compressibility is one of the key phenomena.

The basic kinematical assumptions of a compressible version of the Leonov model are briefly discussed. The prime assumption made by Leonov [5] is that the deformation tensor $\mathbf{F}$, relating the current to the reference configuration, can be multiplicatively decomposed into an elastic ($\mathbf{F}_e$) and a plastic ($\mathbf{F}_p$) part: $\mathbf{F} = \mathbf{F}_e . \mathbf{F}_p$; see Leonov [5, 9] and Stickforth [6]. Secondly it is assumed that the polymer cannot be given a plastic volume change, i.e. $J_p = \det(\mathbf{F}_p) = 1$ and $J_e = \det(\mathbf{F}_e) = \det(\mathbf{F}) = J$.

Following Simo [7], volumetric changes embedded in $\mathbf{F}_e$ are separated from the deviatoric responses by defining the kinematic split

$$\bar{\mathbf{F}}_e = J^{-1/3}\mathbf{F}_e. \tag{3.1}$$

The Finger strain tensors associated with $\mathbf{F}$, $\mathbf{F}_e$ and $\bar{\mathbf{F}}_e$ are

$$\mathbf{B} = \mathbf{F} . \mathbf{F}^c, \qquad \mathbf{B}_e = \mathbf{F}_e . \mathbf{F}_e^c, \qquad \bar{\mathbf{B}}_e = \bar{\mathbf{F}}_e . \bar{\mathbf{F}}_e^c. \tag{3.2}$$

If $\mathbf{L} = (\nabla \mathbf{v})^c$ is the velocity gradient tensor, then $\mathbf{L} = \dot{\mathbf{F}} . \mathbf{F}^{-1}$. It is common practice to decompose $\mathbf{L}$ additively into an elastic and a plastic part:

$$\mathbf{L} = \mathbf{L}_e + \mathbf{L}_p, \qquad \mathbf{L}_e = \dot{\mathbf{F}}_e . \mathbf{F}_e^{-1}, \qquad \mathbf{L}_p = \mathbf{F}_e . \dot{\mathbf{F}}_p . \mathbf{F}^{-1}. \tag{3.3}$$

These are used to define spin ($\mathbf{W}_\alpha$) and deformation rate ($\mathbf{D}_\alpha$) tensors

$$\mathbf{L}_\alpha = \mathbf{D}_\alpha + \mathbf{W}_\alpha, \qquad \mathbf{D}_\alpha^c = \mathbf{D}_\alpha, \qquad \mathbf{W}_\alpha^c = -\mathbf{W}_\alpha \quad (\alpha = -, e, p). \tag{3.4}$$

In accordance with Leonov [5], $\mathbf{W}_p$ is chosen equal to the null tensor. Finally, it can be shown that

$$\dot{\bar{\mathbf{B}}}_e = (\mathbf{L}^d - \mathbf{D}_p) . \bar{\mathbf{B}}_e + \bar{\mathbf{B}}_e . (\mathbf{L}^{dc} - \mathbf{D}_p). \tag{3.5}$$

The Cauchy stress tensor $\boldsymbol{\sigma}$ is split into an elastic part ($\boldsymbol{\sigma}_e$) and a plastic part ($\boldsymbol{\sigma}_p$): $\boldsymbol{\sigma} = \boldsymbol{\sigma}_e + \boldsymbol{\sigma}_p$. First the elastic stresses are defined, then the plastic part is given. Thereafter the temperature dependence of the material parameters is discussed.

Elastic stresses. It is common practice to decompose $\boldsymbol{\sigma}_e$ into a hydrostatic and a deviatoric part: $\boldsymbol{\sigma}_e = -p\mathbf{I} + \boldsymbol{\tau}_e$. In the multi-mode case, the elastic extra stress tensor

τ_e is chosen as

$$\tau_e = \sum_{k=1}^{n} \frac{\eta_k}{\theta_k} \bar{\mathbf{B}}_{ek}^d. \tag{3.6}$$

For each mode k, the unimodular Finger tensor $\bar{\mathbf{B}}_{ek}$ is calculated from (3.5), hence a relation for $\mathbf{D}_{pk}$ needs to be given. By analogy with Leonov's [5] proposal, the following form is chosen:

$$\mathbf{D}_{pk} = \frac{1}{4\theta_k} (\bar{\mathbf{B}}_{ek}^d - \bar{\mathbf{B}}_{ek}^{-d}). \tag{3.7}$$

Substitution of (3.7) into (3.5) yields for each mode k

$$\dot{\bar{\mathbf{B}}}_{ek} = \mathbf{L}^d . \bar{\mathbf{B}}_{ek} + \bar{\mathbf{B}}_{ek} . \mathbf{L}^{dc} - \frac{1}{2\theta_k} \left(\bar{\mathbf{B}}_{ek} . \bar{\mathbf{B}}_{ek} - \mathbf{I} - \tfrac{1}{3}(\mathrm{tr}(\bar{\mathbf{B}}_{ek}) - \mathrm{tr}(\bar{\mathbf{B}}_{ek}^{-1}))\bar{\mathbf{B}}_{ek} \right). \tag{3.8}$$

Note that, in contrast with the incompressible Leonov model, for plane flow $\mathrm{tr}(\bar{\mathbf{B}}_{ek}) \neq \mathrm{tr}(\bar{\mathbf{B}}_{ek}^{-1})$.

A relation for the pressure p remains to be given. This is done implicitly by taking a suitable relation for the specific volume. The so-called Tait equation is a successful model for amorphous polymers (Zoller [10]) and is given below:

$$v(p, T) = (a_0 + a_1(T - T_g)) \left(1 - 0.0894 \ln \left(1 + \frac{p}{B} \right) \right), \tag{3.9}$$

where T_g is the pressure dependent glass transition temperature, i.e. $T_g(p) = T_g(0) + sp$, and $B(T) = B_0 \exp(-B_1 T)$.

Plastic stresses. The plastic part of $\boldsymbol{\sigma}$ is chosen as

$$\boldsymbol{\sigma}_p = 2\eta'(T, p)\mathbf{D}^d. \tag{3.10}$$

Time-temperature superposition. Thermorheological simple behaviour is assumed, implying that

$$\eta_k = a_T(T)\eta_{k0}, \qquad \theta_k = a_T(T)\theta_{k0}, \qquad \eta' = a_T(T)\eta'_0, \tag{3.11}$$

where a_T is the shift factor and η_{k0} and θ_{k0} are the viscosity and relaxation time at a

reference temperature, say T_0. The shift factor is governed by the WLF equation if $T \geqslant T_g$, i.e.

$$\log a_T(T) = \frac{C_1(T - T_0)}{C_2 + T - T_0}, \tag{3.12}$$

while, below T_g

$$a_T(T) = a_T(T_g). \tag{3.13}$$

3.2. Thermal behaviour

To calculate the temperature distribution in the polymer, constitutive equations for the heat flux and the specific internal energy are given.

Heat flux. The heat flux vector $\mathbf{h}$ is assumed to obey Fourier's law, that is

$$\mathbf{h} = -\lambda \nabla T. \tag{3.14}$$

Specific internal energy. Using the results of Stickforth [6] it is easily shown that for the Leonov model the specific internal energy can be written as

$$\rho \dot{\varepsilon} = \boldsymbol{\sigma}_e : (\mathbf{D} - \mathbf{D}_p) - \rho c_v \dot{T} - \frac{\partial \boldsymbol{\sigma}_e}{\partial T} : (\mathbf{D} - \mathbf{D}_p),$$

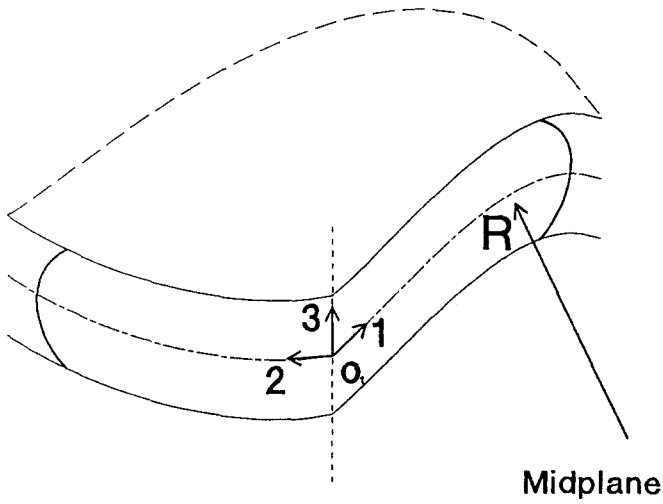

Fig. 1. Definition of the local basis O_1.

where c_v is the specific heat at constant pressure. However, in this paper the energy equation is derived assuming generalized Newtonian material behaviour, where the extra stress tensor $\boldsymbol{\tau}$ is written as $\boldsymbol{\tau} = 2\bar{\eta}\mathbf{D}^d$, with $\bar{\eta}$ the steady state viscosity of the Leonov model. In this case, Sitters [2] has shown that

$$\dot{\varepsilon} = c_p \dot{T} - pv\,\mathrm{tr}(\mathbf{D}) - T\frac{\partial v}{\partial T}\dot{p}, \tag{3.15}$$

where c_p is the specific heat at constant pressure. Hence, the energy equation is written as

$$\rho c_p \dot{T} = \nabla . \lambda \nabla T + \boldsymbol{\tau} : \mathbf{D}^d - \frac{T}{\rho}\frac{\partial \rho}{\partial T}\dot{p}. \tag{3.16}$$

4. Thin film approximation

4.1. Introduction

In this section the set of balance equations and constitutive equations of the previous sections are simplified considerably by introducing a number of geometrical assumptions. Only narrow, weakly curved cavities are considered such that the thin film approximation holds (see Fig. 1). For generalized Newtonian material behaviour this procedure is well described in for example, Sitters [2]. Here a viscoelastic material model is used. Still the assumption that shear flow dominates is adopted.

Preliminaries. At each point $\mathbf{x}_R$ of the midplane R, a local orthonormal basis $O_1 = \{\mathbf{e}_1, \mathbf{e}_2, \mathbf{e}_3\}$ can be defined, such that $\mathbf{e}_1$ and $\mathbf{e}_2$ are tangent to R, and $\mathbf{e}_3$ is normal to R, e.g. $\mathbf{e}_3 = \mathbf{n}$. The position vector of a particle along $\mathbf{n}$ that emanates from $\mathbf{x}_R$ is denoted by $\mathbf{x}$. Now, let $\mathbf{A}$ be an arbitrary second order tensor and $\mathbf{a}$ some vector, then the components of $\mathbf{A}$, respectively $\mathbf{a}$, with respect to O_1 follow from $A_{ij} = \mathbf{A} : \mathbf{e}_j\mathbf{e}_i$, respectively $a_i = \mathbf{a} . \mathbf{e}_i$, $i = 1, 2, 3$.

4.2. Pressure problem

Assumptions

1. With respect to O_1, it is assumed that the contribution of the normal stresses in the momentum equation can be neglected. This can be made plausible by noting that gradients in the thickness direction are far superior to the in plane gradients.
2. The pressure is independent of the $\mathbf{e}_3$ direction.
3. Thermal conduction tangent to the midplane R is neglected.

Due to these assumptions the momentum equation is approximated by (with respect to O_1)

$$\underline{\nabla} p = \frac{\partial}{\partial x_3} \underline{\tau}, \tag{4.1}$$

$$p = p(x_1, x_2), \tag{4.2}$$

with

$$\underline{\nabla}^T = \left[\frac{\partial}{\partial x_1} \quad \frac{\partial}{\partial x_2} \right] \quad \text{and} \quad \underline{\tau}^T = [\tau_{13} \quad \tau_{23}]. \tag{4.3}$$

The above approximation is often referred to as the thin film or lubrication theory. Employing the viscoelastic model (3.6) it follows from $\boldsymbol{\sigma} = \boldsymbol{\sigma}_e + \boldsymbol{\sigma}_p$, $\boldsymbol{\sigma}_e = -p\mathbf{I} + \boldsymbol{\tau}_e$ and (3.10) that

$$\tau_{i3} = \eta' \frac{\partial v_i}{\partial x_3} + \tau^e_{i3}, \qquad \tau^e_{i3} = \sum_{k=1}^{n} \frac{\eta_k}{\theta_k} \bar{\mathbf{B}}^d_{ek} : \mathbf{e}_3 \mathbf{e}_i, \qquad i = 1, 2. \tag{4.4}$$

With respect to O_1 the continuity equation (2.1) is written as

$$\underline{\nabla}^T \underline{v} + \frac{\partial v_3}{\partial x_3} = -\frac{\dot{\rho}}{\rho}, \qquad \underline{v}^T = [v_1 \quad v_2]. \tag{4.5}$$

From this the so-called pressure problem can be derived (see Appendix A):

PE Given $T(\mathbf{x}, t)$, find $p(x_1, x_2, t) \geqslant 0$ such that

$$\underline{\nabla}^T (S \underline{\nabla} p + \hat{\underline{\tau}}) = -\int_{s^-}^{s^+} \frac{\dot{\rho}}{\rho} \mathrm{d}x_3 - \frac{\mathrm{d}h}{\mathrm{d}t}, \quad (p \geqslant 0), \tag{4.6}$$

$$S = -J_2 + \frac{J_1^2}{J_0}, \qquad J_i = \int_{s^-}^{s^+} \frac{x_3^i}{\eta'} \mathrm{d}x_3, \quad (i = 0, 1, 2), \tag{4.7}$$

$$\hat{\underline{\tau}}^T = [\hat{\tau}_{13} \quad \hat{\tau}_{23}], \qquad \hat{\tau}_{i3} = -\frac{J_1}{J_0} \int_{s^-}^{s^+} \frac{\tau^e_{i3}}{\eta'} \mathrm{d}x_3 + \int_{s^-}^{s^+} \frac{x_3 \tau^e_{i3}}{\eta'} \mathrm{d}x_3, \quad (i = 1, 2). \tag{4.8}$$

In this, S is the so-called fluidity coefficient, and s^+ and s^- denote the locations of the solidified layers. Further $\hat{\underline{\tau}}$ represents the contribution of elastic effects, $\int_{s^+}^{s^+} \dot{\rho}/\rho \, \mathrm{d}x_3$ represents compressibility and $\mathrm{d}h/\mathrm{d}t$ accounts for mould elasticity. Note that for symmetric flow $J_1 = 0$. The pressure p is not allowed to drop below zero, because as soon as p becomes zero the material loses contact with the mould.

Equation (4.6) is taken as a starting point for the finite element implementation. Various aspects of this implementation can be found in for example, Sitters [2].

4.3. Temperature equation

With the use of (3.14) and (3.15) the energy equation (2.2) is written as

$$\rho c_p \dot{T} = \nabla . \lambda \nabla T + \boldsymbol{\tau} : \mathbf{D}^d - \frac{T}{\rho}\frac{\partial \rho}{\partial T}\dot{p}. \tag{4.9}$$

To take dissipation into account without having to deal with viscoelastic phenomena, $\boldsymbol{\tau}$ in (4.9) is taken to represent the generalized Newtonian behaviour of the material. Hence $\boldsymbol{\tau} = 2\bar{\eta}(\dot{\gamma}, T)\mathbf{D}^d$, where $\dot{\gamma}$ is the shear rate ($\dot{\gamma} = \sqrt{2\mathbf{D}^d : \mathbf{D}^d}$). The viscosity $\bar{\eta}$ is obtained from the steady state behaviour of the incompressible Leonov model [5] at simple shear

$$\bar{\eta}(\dot{\gamma}, T) = \eta' + \sum_{k=1}^{n} \frac{2\eta_k}{1 + x_k}, \qquad x_k = \sqrt{(1 + 4\dot{\gamma}^2 \theta_k^2)}. \tag{4.10}$$

Further, the conduction along the channel is neglected due to the thinness of the cavity compared to it's length. Hence with respect to O_1, the temperature problem to be solved is

PT Given $\mathbf{v}(\mathbf{x}, t)$ and $p(x_1, x_2, t)$, find $T(\mathbf{x}, t)$ such that

$$\rho c_p \dot{T} = \frac{\partial}{\partial x_3}\left(\lambda \frac{\partial T}{\partial x_3}\right) + \bar{\eta}\dot{\gamma}^2 - \frac{T}{\rho}\frac{\partial \rho}{\partial T}\dot{p}. \tag{4.11}$$

5. Computational aspects

In all cases the implicit Euler scheme is used for temporal discretization. At each time step first the temperature and pressure equation are solved independently, where coupling is enforced by the iterative scheme. That is, the sequence of problems to be solved at each time step is: **PT** → **PE** → **PT** → **PE** → ⋯ until convergence. The pressure problem **PE** is solved by employing the Finite Element Method (FEM) with linear elements. The non-linearity of the resulting set of equations is dealt with in this section. The temperature problem **PT** is solved with a Finite Difference (FD) scheme where the differential grid is centered at each element. Four computational aspects are dealt with in more detail: the solution of the pressure problem **PE**, the method of characteristics to handle the material derivatives, the calculation of the shear rate in case of viscoelastic material behaviour, and the calculation of $\bar{\mathbf{B}}_{ek}$.

Solution of the pressure problem. The system of equations (4.6) is highly non-linear and is solved with a two step procedure. A fully implicit scheme is used in the time domain.

Step 1. An initial estimate for the pressure p, and associated properties such as velocity and shear rate fields, are found by solving for generalized Newtonian material behaviour. The viscosity is taken as the steady state viscosity of the incompressible Leonov model. Then **PE** reduces to

PV Given $T(\mathbf{x}, t)$, find $p(x_1, x_2, t) \geqslant 0$ such that

$$\nabla^T(\bar{S}\nabla p) = -\int_{s^-}^{s^+} \frac{\dot{\rho}}{\rho} \mathrm{d}x_3 - \frac{\mathrm{d}h}{\mathrm{d}t}, \quad (p \geqslant 0), \tag{5.1}$$

$$\bar{S} = -\bar{J}_2 + \frac{\bar{J}_1^2}{\bar{J}_0}, \qquad \bar{J}_i = \int_{s^-}^{s^+} \frac{x_3^i}{\bar{\eta}} \mathrm{d}x_3, \quad (i = 0, 1, 2). \tag{5.2}$$

Equation (5.1) is solved with a Picard iteration scheme, assuming $\mathrm{d}h/\mathrm{d}t = 0$

$$\int_{s^-}^{s^+} \left(\frac{1}{\rho}\frac{\partial \rho}{\partial p}\right)^i \mathrm{d}x_3 \dot{p}^{i+1} + \nabla^T(\bar{S}^i \nabla p^{i+1}) = -\int_{s^-}^{s+} \left(\frac{\dot{\rho}}{\rho}\right)^i \mathrm{d}x_3 + \int_{s^-}^{s^+} \left(\frac{1}{\rho}\frac{\partial \rho}{\partial p}\right)^i \mathrm{d}x_3 \dot{p}^i, \tag{5.3}$$

$$\bar{S}^i = -\bar{J}_2^i + \frac{\bar{J}_1^{2i}}{\bar{J}_0^i}, \qquad \bar{J}_j^i = \int_{s^-}^{s^+} \frac{x_3^j}{\bar{\eta}^i} \mathrm{d}x_3, \quad (j = 0, 1, 2), \tag{5.4}$$

where the superscripts i and $i + 1$ respectively refer to the previous or the current iteration.

Step 2. Given an estimate of the pressure, shear rate field, etc. by step 1, **PE** is finally solved with the Newton iteration process. Within the finite element context, the element stiffness matrices are determined by numerical differentiation.

Method of characteristics (Pironneau [11] and Morton et al. [12]). Consider the time interval $t \in [t_n, t_{n+1}]$, and let $\Delta t = t_{n+1} - t_n$. The time derivative $\dot{p}$ is approximated by

$$\dot{p} = \frac{p(\mathbf{x}, t_{n+1}) - p(\mathbf{s}_n, t_n)}{\Delta t}, \tag{5.5}$$

where $\mathbf{s}_n$ designates the position at time t_n of the material particle currently located at $\mathbf{x}$. The material time derivatives of T and $\bar{\mathbf{B}}_{ek}$ are treated likewise.

Calculation of the shear rate. To calculate $\bar{\mathbf{B}}_{ek}$, the shear rate needs to be known. Equation (A.2) constitutes a non-linear relation for the shear rate. It is solved pointwise with a secant-method, such that $\bar{\mathbf{B}}_{ek}$ and $\partial v/\partial x_3$ are calculated simultaneously.

Calculation of $\bar{\mathbf{B}}_{ek}$. The k'th mode unimodular elastic Finger strain tensor $\bar{\mathbf{B}}_{ek}$ is calculated from (3.8). A variable-order variable-time step backward difference scheme

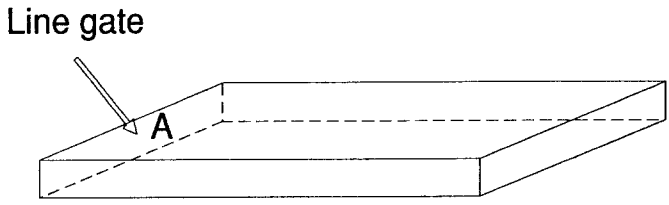

Fig. 2. Sketch of the cavity, strip of $80 \times 50 \times 2$ mm.

is used to integrate (3.8) over a certain time interval. During each time interval, say $t_n \rightarrow t_{n+1}$, $\mathbf{L}$ is assumed constant and the initial value of $\bar{\mathbf{B}}_{ek}$ is $\bar{\mathbf{B}}_{ek}(\mathbf{s}_n, t_n)$.

6. Example

As an example polystyrene (PS) is injected into a cavity of $80 \times 50 \times 2$ mm (length, width, height), see Fig. 2. Along A a line gate is assumed. The material properties of PS in case a viscoelastic constitutive model is used are given in Table 1. Mould elasticity is neglected in this example.

Processing conditions PS. The material is injected with an average velocity of 120 mm/s at 200°C. This velocity is maintained at A until the holding pressure of

Table 1. Parameters for PS

Parameters WLF equation: (from Isayev et al. [4])
$T_0 = 134$°C
$C_1 = -8.86$
$C_2 = 101.6$°C

Thermal properties: (from Isayev et al. [4])
$c_p = 1840$ J/(kg K)
$\lambda = 0.13$ J/(sm K)

Visco-elastic properties: (from Flaman [14])
$\eta' = 0.08795$ MPas
$\theta_1 = 1147$ s $\quad \eta_1 = 7.5908$ MPas
$\theta_2 = 38.71$ s $\quad \eta_2 = 2.0930$ MPas

Tait parameters: (from Zoller [10])
$s = 0.51$°C/MPa
$T_g(0) = 100$°C

solid	melt
$a_0 = 972$	972 mm^3/g
$a_1 = 0.224$	0.544 mm^3/gK
$B_0 = 353.4$	252.1 MPa
$B_1 = 2.999\ 10^{-3}$	$4.08\ 10^{-3}$°C^{-1}

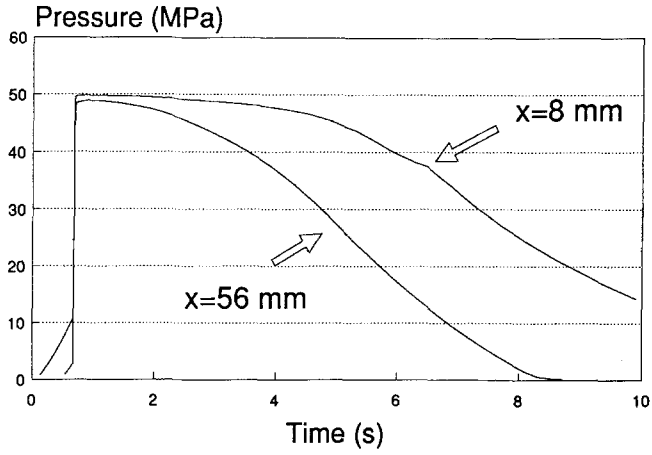

Fig. 3. Numerical pressure trace for PS, viscoelastic material model.

50 MPa is reached. The holding pressure is maintained at A until all material at A has solidified. The mould has a temperature of 50°C.

Results for PS. Calculations were done with both the viscoelastic and the viscous model. Figure 3 shows the calculated pressure history at $x_1 = 8$ mm and $x_1 = 56$ mm for the viscoelastic case. They virtually coincide with the results of the viscous model. During the filling of the mould, for $t \in [0, t_f = 0.67]$ s, the pressure gradually rises. Then a short compression stage follows where the pressure rapidly increases to 50 MPa. Hereafter, due to cooling, the pressure slowly decays, until at time $t_{gf} = 6.3$ s

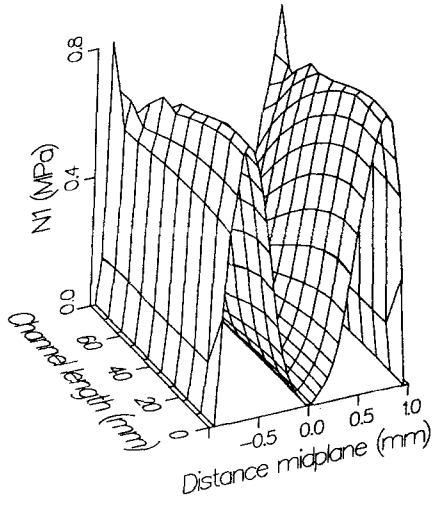

Fig. 4. N_1 at end of filling stage, $t = 0.67$ s.

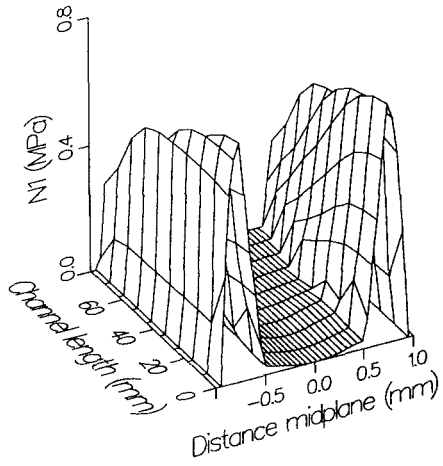

Fig. 5. N_1 at end of compression stage.

the gate has solidified completely. After solidification of the gate the pressure decays further until the product is ejected from the mould.

In Figs. 4–8 the evolution of the first normal stress difference N_1, defined as $N_1 = \tau^e_{11} - \tau^e_{33}$, for the viscoelastic (direct) case is shown. N_1 is shown at 5 times: at the end of the filling stage $t_f = 0.67$ s, at the end of the compression stage $t_c = 0.71$ s, and at $t_c + 1.5$, $t_c + 3.0$ and $t_c + 6.0$ s. During the compression stage most of the flow induced normal stresses relax because the flow rate is low and the temperature at the core of the cavity is still quite high, compare Figs. 4 and 5. This does not apply to regions close to the walls, because there the temperature has dropped below T_g and relaxation is virtually stopped. During the post-filling stage shear rates are orders of

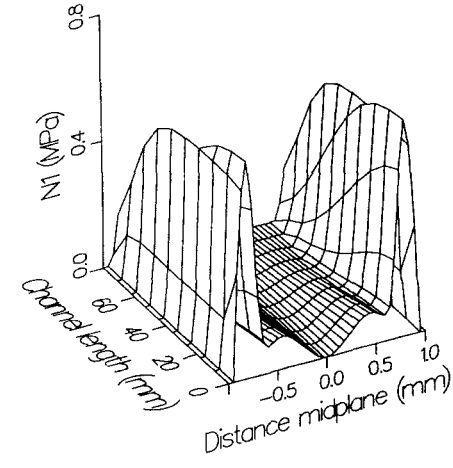

Fig. 6. N_1 at $t = 2.21$ s.

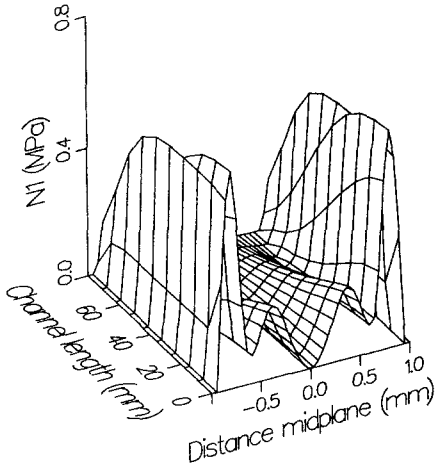

Fig. 7. N_1 at $t = 3.71$ s.

magnitude smaller than in the filling stage. However, due to the decreasing temperature as time proceeds, small shear rates may still introduce considerable normal stresses as is clearly demonstrated in Figs. 5–8. Figure 8 shows the final N_1 distribution because at that time all material has solidified.

These results can be compared with calculations obtained with the *indirect* method, where the kinematics of the generalized Newtonian model is used to calculate flow induced residual stresses with the compressible Leonov model. The N_1 distribution thus obtained after solidification of the entire product is shown in Fig. 9. Figures 10 and 11 compare N_1 obtained with both techniques at two different locations in the mould. Qualitatively the results are in very good agreement, while the computation time of the indirect method is less than 1/10 of the direct method.

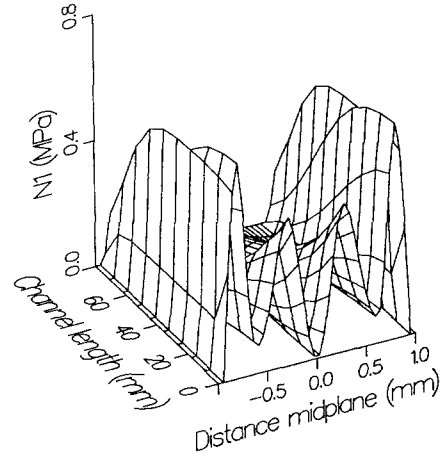

Fig. 8. N_1 at $t = 6.71$ s.

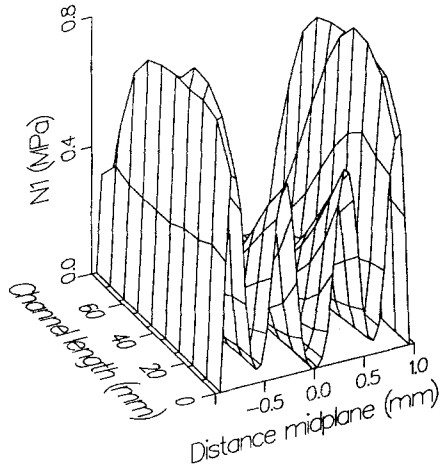

Fig. 9. N_1 according to the indirect model.

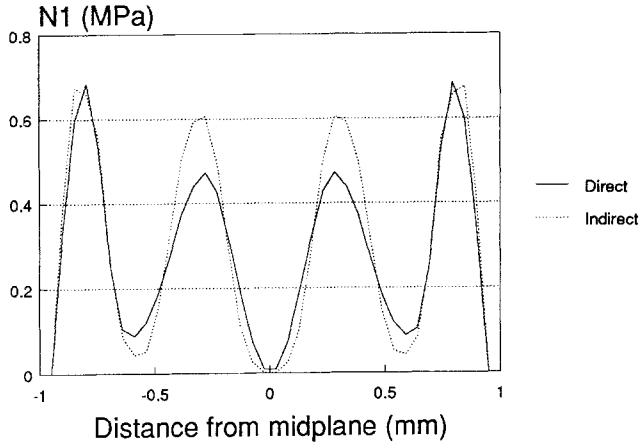

Fig. 10. Comparison of N_1 at $x_1 = 0$ mm.

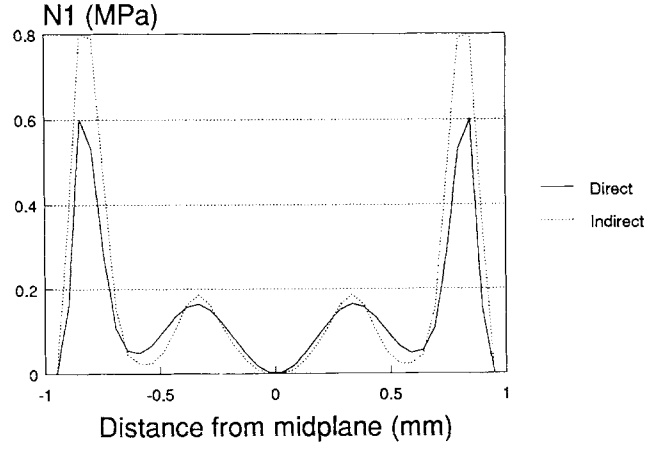

Fig. 11. Comparison of N_1 at $x_1 = 40$ mm.

7. Conclusions

The evolution of flow induced stresses during injection moulding in both the filling and the post-filling stage is investigated numerically. A compressible version of the Leonov model was developed and applied.

The calculations clearly show that a substantial portion of the flow induced residual stresses arise during the post-filling stage. This is in agreement with experimental data [13]. The direct (viscoelastic) approach does not significantly differ (results mostly agree within 10%) from the much cheaper indirect method. In this latter method the pressure problem is derived with generalized Newtonian material behaviour, and the resulting kinematics is supplied to the viscoelastic constitutive equation. This approach is a valuable tool to give a quick and fairly accurate indication of the molecular orientation in an injection moulded product (provided that one assumes that flow induced stresses are a measure of molecular orientation).

Appendix A. Derivation of the pressure problem

Substitution of (4.4) into (4.1) gives

$$\underline{\nabla} p = \frac{\partial}{\partial x_3}\left(\eta' \frac{\partial \underline{v}}{\partial x_3} + \underline{\tau}^e\right), \qquad \underline{\tau}^{eT} = [\tau^e_{13} \quad \tau^e_{23}]. \tag{A.1}$$

Step 1. Integrating (A.1) with respect to x_3 yields (note that $p = p(x_1, x_2)$)

$$\frac{\partial \underline{v}}{\partial x_3} = \frac{1}{\eta'}(x_3 \underline{\nabla} p + \underline{c} - \underline{\tau}^e), \tag{A.2}$$

where $\underline{c}$ is an integration constant column.

Step 2. The velocity $\underline{v}$ is found by integrating (A.2) from s^- to x_3

$$\underline{v} = \int_{s^-}^{x_3} \frac{\partial \underline{v}}{\partial x_3} \mathrm{d}x_3 = \int_{s^-}^{x_3} \frac{1}{\eta'}(x_3 \underline{\nabla} p + \underline{c} - \underline{\tau}^e) \mathrm{d}x_3. \tag{A.3}$$

This holds because at $x_3 = s^- \underline{v} = \underline{0}$. Because $\underline{v} = \underline{0}$ at $x_3 = s^+$ as well, it follows that

$$\underline{c} = -\frac{J_1}{J_0} \underline{\nabla} p + \frac{1}{J_0} \int_{s^-}^{s^+} \frac{\underline{\tau}^e}{\eta'} \mathrm{d}x_3. \tag{A.4}$$

Step 3. Integrating the velocity with respect to x_3 once more gives (after repeated use of $\int fg_{,x}\,dx = fg - \int f_{,x}g\,dx$)

$$\int_{s^-}^{s^+} \underset{\sim}{v}\,dx_3 = \left(-J_2 + \frac{J_1^2}{J_0}\right)\underset{\sim}{\nabla} p - \frac{J_1}{J_0}\int_{s^-}^{s^+} \frac{\underset{\sim}{\tau}^e}{\eta'}\,dx_3 + \int_{s^-}^{s^+} \frac{x_3 \underset{\sim}{\tau}^e}{\eta'}\,dx_3. \tag{A.5}$$

Step 4. Integration of the continuity relation (4.5) from s^- to s^+, the use of (A.5) and the recognition that

$$\frac{dh}{dt} = \int_{s^-}^{s^+} \frac{\partial v_3}{\partial x_3}\,dx_3 = v_3(s^+) - v_3(s^-) \tag{A.6}$$

gives the final result.

References

1. Boshouwers, G. and Werf, J.v.d., Inject-3, a simulation code for the filling stage of the injection moulding process of thermoplastics. Ph.D. Thesis, Eindhoven Univ. Technology (1988).
2. Sitters, C., Numerical simulation of injection moulding. Ph.D. Thesis, Eindhoven Univer. Techn. (1988).
3. Manzione, L.T., *Application of Computer Aided Design in Injection Molding.* Hanse Publ. (1988).
4. Isayev, A.I. and Hieber, C.A., Toward a viscoelastic modelling of the injection molding of polymers. *Rheologica Acta* (1980) 168–182.
5. Leonov, A.I., Nonequilibrium thermodynamics and rheology of viscoelastic polymer media. *Rheologica Acta* 15 (1976) 85–98.
6. Stickforth, J., The rational mechanics and thermodynamics of polymeric fluids based upon the concept of a variable reference state. *Rheologica Acta* 25 (1986) 447–458.
7. Simo, J.C., On a fully three dimensional finite strain viscoelastic damage model: formulation and computational aspects. *Comp. Meth. Appl. Mech. Eng.* 60 (1987) 153–173.
8. Upadyay, R.K., Isayev, A.I. and Shen, S.F., Transient shear flow behaviour according to the Leonov model. *Rheologica Acta* 20 (1981) 443–457.
9. Leonov, A.I., On a class of constitutive equations for viscoelastic liquids. *Jrnl. Non-Newt. Fl. Mech.* 15 (1987) 1–59.
10. Zoller, P., A study of the pressure-volume-temperature relationships of four related amorphous polymers: polycarbonate, polyarylate, phenoxy and polysulfone. *Jrnl. Pol. Sc.* 20 (1982) 1453–1464.
11. Pironneau, O., On the transport-diffusion algorithm and its application to the Navier–Stokes equation. *Numer. Math.* 38 (1982) 309–332.
12. Morton, K.W., Priestly, A. and Suli, E., Stability analysis of the Lagrange–Galerkin method with non-exact integration. Oxford University Computing Laboratory, Report 86/14 (1986).
13. Wimberger-Friedl, R. and Janeschitz-Kriegl, H., Residual birefringence in Compact Discs, submitted for publication (1989).
14. Flaman, A., Personal communication.
15. Isayev, A.I. and Hariharan, T., Volumetric effects in the injection molding of polymers. *Pol. Eng. and Science* 25 (1985) 271–277.